RESEARCH ARTICLE

Arun Dev Sharma
Amrita Chauhan
Inderjeet Kaur

Bio-active components of *Melaleuca alternifolia, Rosmarinus officinalis, Boswellia serrata* essential oil as anti-diabetic therapeutics targeting α-amylase : *In vitro* α-amylase inhibition, antioxidant, binding interaction, and docking studies of predominant compounds

Authors' addresses:
P.G Dept of Biotechnology, Lyallpur Khalsa College, Mohyal Nagar Jalandhar, Punjab (144008), India

Correspondence:
Arun Dev Sharma
P.G Dept of Biotechnology, Lyallpur Khalsa College, Mohyal Nagar Jalandhar, Punjab (144008), India
e-mail adslkcjal@gmail.com

Article info:
Received: 1 April 2024
Accepted: 28 May 2024

ABSTRACT

Tea tree essential oil (TEO), Rosemary Essential Oil (REO), and Guggul essential oil (GEO) (EOs) are priceless essential oils that have been linked to several biological activities, including antibacterial, antifungal, immunomodulatory, anticancer, and anti-inflammatory effects. α-amylase inhibition is a hopeful curative target against type-2 diabetes as it can downgrade fierce digestion and absorption of carbohydrates into absorbable monosaccharides. The purpose of the study is *in silico* molecular docking of principal components of TEO, REO, and GEO followed by *in vitro* validation of inhibition of α-amylase activity.

For docking Cb-dock2 tool was utilized. Ligand-Protein 2-D interactions were also studied. From the perspective of human health, *in silico* ADMET pharmacoinformatic features (Physicochemical, Lipophilicity, Medicinal Chemistry, Druglikeness, Absorption, Water Solubility, Distribution, Metabolism, Pharmacokinetics, Excretion) have prospected. Using α-amylase, wet lab validation was carried out. 2, 2-Diphenyl-1-picryl hydrazyl (DPPH) radical inhibition assay was conducted to ascertain the antioxidant role of all EOs.

Docking investigation demonstrated the effective binding of all the ligands with the α-amylase. The interaction results imply that the enzyme-ligand complexes form hydrogen, hydrophobic, and other interactions. *In silico* ADMET examination disclosed that all the ligand molecules have no toxic effect and acceptable absorption, as well. Further, TEO, REO, and GEO have dose-dependent inhibitory action against α-amylase. All EOs depicted good antioxidant potential. Kinetic analysis revealed that TEO, REO, and GEO competitively inhibited α-amylase.

It was concluded that these substances can function as model molecules for the synthesis of novel anti-diabetic substances.

Key words: α-amylase; diabetes; essential oil; molecular docking; Acarbose

Introduction

Type-2 diabetes mellitus (T2DM) is the major problem worldwide which is related to postprandial or post-meal hyperglycemia (Alema et al., 2020). Earlier data suggested that more than 400 million adults experienced diabetes worldwide in 2014 and is estimated to reach 330 million in 2030 (Lolok et al., 2022). A major objective of diabetes treatment is to reduce postprandial hyperglycemia, which is a hallmark of type-2 diabetes (Smita et al., 2018). Hence, it has become a major medical problem worldwide. The presence of glucose in the bloodstream during prolonged hyperglycemia is linked to protein (glycation), which can have serious repercussions, including altered protein function, robust aggregation, and changes in absorption peaks in the lens, which can lead to opacification and cataracts, particularly in individuals with diabetes. Moreover, glycation may be connected to brain damage and Alzheimer's disease, among

http://www.jbb.uni-plovdiv.bg DOI: 10.69085/jbb20241001

other age-related illnesses. Also, cells may be harmed by glucose's binding to DNA (Dalli et al., 2022). High blood sugar can cause serious consequences such as microvascular changes (brain infarction, coronary artery disease, and arterial disease) and macrovascular changes (neuropathy, retinal degeneration, and nephropathy) if left untreated (El Moussaoui et al., 2021; Bhaskarachary et al., 2018). Nutritional treatments are often recommended to improve postprandial hyperglycemia in early-stage diabetes patients by reducing the glucose release from digesting carbohydrates before being recommended for pharmacologic treatment (Ch'ng et al. 2019). Various enzymes including α-amylase (1,4-α-d-glucan-glucanohydrolase, EC 3.2. 1.1), which is found in saliva and pancreatic juice, is the key enzyme involved in carbohydrate digestion, which recreates a critical role in breaking down starch into maltose and glucose (Lolok et al., 2022). Thus, inhibitors of the enzyme α-amylase that slow down carbohydrate digestion and consequently reduce the circulation of glucose in the blood are considered viable and beneficial treatments for reducing the risk of developing diabetes (Kazeem et al., 2013). Acarbose, voglibose, and miglitol are a few well-established synthetic medications for diabetes that are well-known for their diverse adverse effects such as bloating, diarrhea, and abdominal pain (Derosa & Meffioli, 2012). It is necessary to look for novel treatment strategies to regulate postprandial glucose levels because commercially existing anti-diabetic medications have unfavorable side effects (McCoy et al., 2020). Plant-based natural α-amylase inhibitors have gained importance in the treatment T2DM due to their affordability, efficacy, and reduced side effects and efficacy (Elwekeel et al., 2022). Inhibiting α-amylase is now being researched as a therapeutic approach. As a result, it's thought that the bioactive compounds in medicinal plants have few or no negative effects (Unuofin & Lebelo, 2020). Many alpha-amylase inhibitors have been found in herbal plants and are expected to be effective replacements for the produced drugs that are already on the market with less adverse effects (Kazeem et al., 2013). Inhibiting α-amylase can considerably lessen the rise in blood glucose that occurs after a meal, making it a useful tactic for controlling blood glucose levels in T2DM patients. Thus, there is a great deal of promise for developing novel drugs to treat diabetes by screening medicinal plants for the inhibition of carbohydrate hydrolases (Smita et al., 2018). Essential oils from plants are a volatile, concentrated, hydrophobic mixture of biochemicals. Many bioactive substances, which are present in essential oils, are reported with pharmacological effects, such as antibacterial, anti-diabetic, anti-cancer, antioxidant, and anti-inflammatory qualities (Mir et al., 2022).

Melaleuca alternifolia, is also known as the Australian tea tree plant of myrtaceae family (Ismail et al., 2022). This plant has strong therapeutic potential. Essential oil from this plant (designated as TEO) has immense use as a therapeutic agent due to the presence of numerous bioactive components (Ismail et al., 2022). *Rosmarinus officinalis* belongs to *Lamiaceae* family (Nieto et al., 2018). Because it protects the brain from free radicals, this plant has a long history of being associated with memory enhancement and has even been employed as a symbol of recollection. Essential oil from this plant (designated as REO) has many therapeutic effects due to the richness of biologically active monoterpenes (de Macedo et al., 2020). *Boswellia serrata*, an ayurveda's ancient and most holy herb is a medium-sized, branching tree that belongs to the family Burseraceae (Bogavac et al., 2022). *Boswellia serrata exudate is an oleo gum-resin also known as* Guggul (Alraddadi et al., 2022) which yields essential oil. Essential oil from this plant (designated as GEO) has been utilized in traditional medicine from the earliest days of time (Hussain et al., 2013). Essential oils (EOs) are concentrated volatile mixtures of polyphenolic-rich biochemicals that possess various biological activities like – antioxidant, anti-microbial, anti-cancer, anti-inflammatory, etc. EO's may provide a substitute for the difficulties related to synthetic hypoglycemic inhibitors. It is thought that their mediated effects in treating pathological conditions occur through a variety of mechanisms, such as enzymatic interactions (modulatory effects) and reactive species scavenging activities (Nimse & Pal, 2015). Additionally, their pharmacological activities are thought to be associated with fewer or no side effects (Elshama et al., 2018; Oboh et al., 2012). If left unchecked, diabetic individuals with high levels of endogenously produced reactive species may also be vulnerable to oxidative damage to certain physiological macromolecules or tissue proteins (Derosa et al., 2020). When phenolic-rich herbal derivatives with mild hypoglycemia and antioxidant potentials are used to treat these individuals, it may be more beneficial for them than only using synthetic hypoglycemic medications (Farombi et al., 2020; Derosa et al., 2020).

All things considered, our earlier phytochemical-based research showed that primary bioactive components of Tea tree essential oil (TEO) are α-terpineol, tetrahydro-3-methyl-5-oxo-2 furan carboxylic acid, 2-oxo-1,8-cineole; Rosemary Essential Oil (REO) are 3-hexanol, camphene, vertocitral and GEO (Guggul essential oil) are: caryophyllene alcohol, octanol, limonene (Sharma et al., 2023a, 2023b, 2023c). A comprehensive study on *Melaleuca alternifolia*, *Rosmarinus officinalis*, and *Boswellia serrata* has not yet been carried out, despite their traditional therapeutic claim. There aren't many reports on the plant's pharmacological properties. It has been demonstrated that several natural compounds possess anti-α-amylase properties, albeit the precise mode of action remains unclear. Analyzing the results of numerous *in vitro*

investigations showed that the use of EOs as antidiabetic medications is intricate and difficult, requiring the necessity for timely study. This study postulated that the numerous bioactive ingredients in TEO, REO, and GEO may be able to lessen the effects of diabetes. Consequently, more investigation is required to ascertain the therapeutic benefits and probable mechanisms of action of essential oils from the aforementioned strategies. In light of everything said above, the objective of the current study was to evaluate an *in silico* analysis of the most prevalent compounds against target enzyme α-amylase involved in the digestion of carbohydrates the *in vitro* amylase activity of pure TTEO, REO, and GEO as well as. It will also provide fresh perspectives to prospective forecasts for determining the most important anti-diabetic medications at dose.

Materials and Methods

Essential oils

For the current investigation, TEO, REO, and GEO essential oils from Melaleuca alternifolia, Rosmarinus officinalis, Boswellia serrata, respectively, were chosen. The present investigation's essential oils were graciously provided by Wommune, Bioryca healthcare Pvt Ltd, India.

Preparation of Ligands

Based on our previous studies (Sharma et al., 2023a, 2023b, 2023c), major along with minor bioactive components viz; TEO: α-terpineol, tetrahydro-3-methyl-5-oxo-2 furan carboxylic acid, 2-oxo-1,8-cineole, REO: 3-hexanol, camphene, vertocitral and GEO: caryophyllene alcohol, octanol, limonene were chosen as ligands for molecular docking studies. SMILES of all eight selected ligands were retrieved from the PubChem (https://pubchem.ncbi.nlm.nih.gov/). Acarbose was used as a standard drug or inhibitor. 3-D structures of ligands were prepared by retrieving SMILES from the NCBI-PubChem database and by using UCSF-chimera.

Target protein preparation

The crystal structures of the enzyme's amylase (PDB ID: 3bai) served as the study's target. The RCSB-PDB database, which can be accessed at https://www.rcsb.org, provided the sources for their structures. Target enzyme receptors were built up for docking research using the Chimera dock prep system. In the optimization process known as dock prep, irregularities in atomic bond length, structure, and charge are corrected.

Molecular Docking study

Molecular docking was done using Cb-dock2 (https://cadd.labshare.cn/cb-dock2/php/index.php) to study the binding mechanism of all the bioactive substances chosen as ligands from TEO, REO, and GEO with α-amylase. Docking was executed by uploading the ligand and target enzyme molecules in a .pdb file to the cb-dock2 tool. The best-generated model in the .pdb file is downloaded and saved. The enzyme-ligand 2-D interactions were predicted by using the Biovia 2020 and UCSF Chimera tools.

Drug-likeness

Physiochemical studies of all the ligands and ADMET (Absorption, Metabolism, Toxicity, and Excretion) examinations were performed using SWISSADME. The bioactivity potential was calculated using the Way2Drug tool (https://www.way2drug.com/passonline/) application.

Active site Prediction

The enzyme α-amylase active sites were predicted using the Computed Atlas of Surface Topography of Proteins (CASTp). A probe radius calculation with a default value of 1.4Å was used to measure and identify cavities on 3-D enzyme structures.

Investigation of molecular interaction between α-amylase and EOs

Interaction between EO's and α-amylase using Ultraviolet (UV)-visible spectroscopy and fluorescence quenching analysis was carried out following Anigboro et al., (2021) with minor modifications.

UV-visible spectral analysis

UV-VIS profile of α-amylase (prepared in 0.5 mg/mL in sodium phosphate buffer, 0.02 M, pH 6.9 and 0.006 M NaCl) was recorded in the range of 200-400 nm at 25°C in the presence of varying concentrations of TEO, REO and GEO (50-250µL) (Labtronics).

Fluorescence quenching analysis

A fluorescence quenching assay was performed at room temperature (20-25°C) at the excitation wavelength of 280 nm with slit bandwidths set at 5 nm. Briefly, 3.5 mL of α-amylase (prepared in 0.5 mg/mL in sodium phosphate buffer, 0.02 M, pH 6.9, and 0.006 M NaCl) was mixed with varying concentrations of TEO, REO, and GEO (50-250µL). The mixture was incubated for 10 min and fluorescence emission spectra were recorded from 250 to 500 nm (Perkin Elmer spectrophotometer, FL6500).

In vitro α-amylase inhibition assay

This experiment was performed using the modified version of the Kazeem et al., (2013); method. Test tubes holding various volumes of EOs (50-250µl) were filled with 0.125ml of α-amylase solution (5 mg/ml) produced in Sodium Phosphate buffer (0.02M, 6.9pH). 500µl of 6.9 pH, 0.02M

buffer was added. The solution was pre-incubated for 10 min in a water bath at 25°C. After adding 0.5 ml of starch solution (2%) prepared in 0.03M sodium phosphate (pH-6.9), the mixture was incubated for 10 min at 25°C. By adding 0.5 ml of DNS reagent, the process was halted. The test tubes were once more placed in a boiling water bath for five min before getting cooled to

ambient temperature. The samples were diluted with 6 ml of sterile distilled water before being measured for absorbance at 540 nm. A standard alpha-amylase inhibitor called acarbose was also utilized as a positive control. When utilized as a control, water was used instead of EOs. The formula used to calculate the level of α-amylase inhibition activity was: % Inhibition=$Abs_{CONTROL}$-$Abs_{EO'S/ACARBOSE}$/$Abs_{CONTROL}$x100.

Determination of mode of Inhibition of α-amylase

According to the following methodology, the course of action of α-amylase inhibition was deduced: 75µl of EO's was pre-incubated at 25 °C for 10 min with 200µl of α-amylase solution (prepared in 0.02M phosphate buffer) and 0.5 ml of 0.02M buffer (6.9pH) in the first batch of test tubes. In the 2nd set of test tubes, 200µl of α-amylase solution was pre-incubated for 10 min at 25°C with 0.5 ml of sodium phosphate buffer (6.9pH, 0.02M). To kick-start the reaction, based on the concentration of the starch solution (1-5 mg/ml) was introduced to each set of test tubes. The final reaction mixture was incubated for 10 minutes at 25°C. The reaction was stopped with the addition of 0.5 ml of DNS reagent, which was followed by a 5-minute incubation period at 100 °C. A typical maltose curve was implemented to quantify the amount of released reducing sugars and their conversion to reaction velocities. A double reciprocal plot between velocity (V_0 and substrate concentration (S) was plotted. The method of inhibition of EO's on α-amylase activity was identified by examining the Lineweaver-Burk plot using Michaelis-Menten kinetics.

In vitro DPPH free radical scavenging activity analysis

With a few minor modifications, the DPPH free radical scavenging activity of TEO, REO, and GEO was assayed as described in Amrita et al. (2023).

Statistical analysis

To find p (<0.05), the Post Hoc Tukey HSD (beta) test was run at https://www.socscistatistics.com/tests/. Every value (n = 3) is the mean ± SD.

Results and Discussion

Previous studies have reported that patients who have uncontrolled sugar levels are prone to T2DM along with other different co-infections due to poor immune systems (Alema et al., 2020). Bioactive compounds having anti-amylase activity are considered key therapeutic molecules. Studies revealed that drugs targeting α-amylase can be promising therapeutic agents to control T2DM (Smita et al., 2018).

Since α-amylase is the key enzyme involved in carbohydrate digestion, it is essential to exploit it as a key target against phytocompounds having α-amylase inhibitory potential. In the light of this observation, the present study was designed to evaluate molecular interactions of TEO, REO, and GEO-based bioactive followed by *in vitro* validation approaches.

Molecular Docking

The current study planned to dock major along with some minor bioactive compounds of TEO: α-terpineol, tetrahydro-3-methyl-5-oxo-2 furan carboxylic acid, 2-oxo-1,8-cineole,

REO: 3-hexanol, camphene, vertocitral and GEO: caryophyllene alcohol, octanol, limonene from *Melaleuca alternifolia*, *Rosmarinus officinalis*, and *Boswellia serrata*, respectively against α-amylase. Acarbose (a well-known inhibitor) as a vital enzyme inhibiting competitors in opposition to α-amylase was also studied. Docking analysis showed that all the bioactive compounds from all EOs efficiently docked with alpha-amylase enzyme (Table 1). The largest potential for inhibition is indicated by bioactive compounds with the lowest vina scores when used with enzymes.

Among all TEO components, the most effective binding was observed with α-terpineol with a docking score of -5.8. In REO, robust binding was observed with camphene having a docking score of -5.5. In GEO, Caryophyllene alcohol depicted strong binding with a docking score of -7.7. The docking data for the α-amylase enzyme showed that acarbose, a common type-2 anti-diabetic medication, demonstrated docking with a vina score of -7.9. Among all EOs, the docking score of caryophyllene alcohol was comparable to that of acarbose.

This shows that the plant EOs are loaded with a variety of phytocompounds that, either used singly or synergistically, decreased the activity of α-amylase as seen in the *in vitro* experimental α-amylase inhibition research.

http://www.jbb.uni-plovdiv.bg DOI: 10.69085/jbb20241001

RESEARCH ARTICLE

Table 1. *Molecular docking of α-amylase with bioactive components of essential oils used as ligands.*

Target enzyme	Ligand		Docking Score			
			Vina Score	Cavity Volume (Å^3)	Center (x, y, z)	Docking Size (x, y, z)
α-amylase PDB ID:3bai	**TEO**	α-terpineol	-5.8	379	8, 18, 67	17, 17, 17
		Tetrahydro-3-methyl-5-oxo-2 furan carboxylic acid	-4.9	379	8, 18, 67	17, 17, 17
		2-oxo-1,8-cineole	-5.7	482	10, 18, 43	16, 16, 16
	REO	3-hexanol	-4.1	482	10, 18, 43	16, 16, 16
		Camphene	-5.5	482	10, 18, 43	16, 16, 16
		Vertocitral	-5.4	482	10, 18, 43	17, 17, 17
	GEO	Caryophyllene alcohol	-7.7	224	6, 29, 34	22, 22, 22
		octanol	-4.5	482	10, 18, 43	19, 19, 19
		Limonene	-5.6	482	10, 18, 43	17, 17, 17
	Acarbose		-7.9	745	-7, -20, 74	27, 27,27

A molecular interaction study was conducted to investigate the potential binding mechanism of our compounds to the α-amylase protein's active site residues. Table 2 provides an illustration of the ligand-target interactions of all bioactive compounds from TEO, REO, and GEO with α-amylase in terms of hydrogen bonds, hydrophobic interactions, and other crucial information. Figure 1 and 2 display the molecular interactions and best docking poses for the eight ligands with α-amylase. Active site predictions revealed residues that interact with the major cavities of the target enzymes, as shown in Table 3. The use of CASTp allowed the identification of a significant pocket in α-amylase with a Volume (SA) of 239.626 and an Area (SA) of 225.493. It was observed that most stable complex in TEO (α-terpineol-α-amylase) was stabilized by 6 alkyl, 4 Van der Waal, 1 Pi-alkyl, interactions involving LYS: 227, PRO: 228, ILE: 230, LEU: 211, PRO: 228, LEU: 214, GLY:249, 251, ASN:250; LYS: 208 and TYR:2 amino acids. Similarly, in REO, the most robust docked structure (camphene- α-amylase) illustrated 1 Pi-sigma, 2 alkyl, 4 Van der Waal and 4 Pi-alkyl bond interactions via TYR:62, LEU:162, LEU:165, ARG:195; ASP:197,300; TRP:59; ALA:198, HIS:101; TYR:32; HIS:299; TRP:58 amino acids. In GEO, Caryophyllene alcohol was docked to α-amylase enzyme via 6 H-bonds, 7 Van der Waal, and 2 C-H bond interactions.

Additionally, docking research demonstrated that acarbose, a well-known inhibitor, interacted with the target enzymes α-amylase via both 9 H- bond 1 alkyl, and 12 Van der Waal interactions. Overall, the inhibitory effect of TEO, REO, and GEO reported in this study was supported by the *in silico* analysis of the ligand-protein interaction of many of the identified compounds in EO's with amino acid residues present in the α-amylase active site domain (such as LEU:162, GLN:63, ARG:195, ALA:198 ASP:300, 197, GLU:233, ALA:198, HIS:101, HIS:101, 299, TYR:62, TRP:58. etc.).

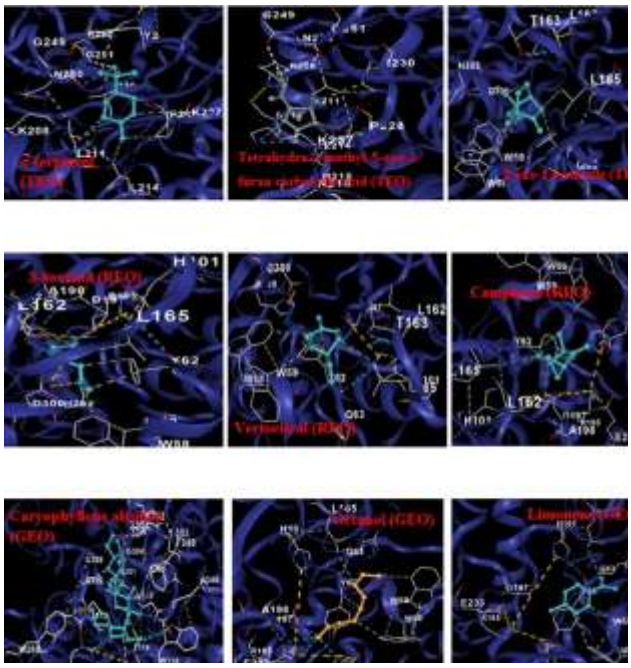

Figure 1. *Docking poses of ligands with α-amylase .*

According to our research, the substances found in the EOs are potentially important metabolites that might regulate the α-amylase enzyme. Our results were in corroboration with Anigboro et al., (2021), citing molecular docking studies of phytochemicals present in *Justicia carnea* extracts with α-amylase enzyme.

http://www.jbb.uni-plovdiv.bg DOI: 10.69085/jbb20241001

Table 2. *Ligand-Enzyme interactions*

Target enzyme		Ligands	Interactions								
			H-Bonds	Pi-sigma	Alkyl	Van der waals	Pi-alkyl	C-H bond	Pi-donor H-bond	Unfavorable donor-donor	Unfavorable acceptor-acceptor
α-amylase	TEO	α-terpineol	___	___	LYS: 227.A, PRO: 228.A, ILE: 230.A, LEU: 211.A, PRO: 228.A, LEU: 214.A	GLY:249,251. A; ASN":250.A; LYS: 208.A	TYR:2. A,	___	___	___	___
		Tetrahydro-3-methyl-5-oxo-2 furan carboxylic acid	LYS:227.A; LYS:227.A	___	LEU:211.A; ILE: 230.A; PRO:228.A	LYS:208.A; HIS:215.A; ASN:216.A; LEU:214.A	___	GLY:249.A; ASN:250.A	___	___	___
		2-oxo-1,8-cineole	GLN:63.A	___	LEU:165.A	LEU:162.A;THR:163.A	TRP:59.A;TYR:62.A;TRP:58.A	___	___	___	___
	REO	3-hexanol	GLU:233.A; ASP:300.A	___	ALA:198.A; LEU:162.A	TRP:59. A; HIS:101.A; ASP:197.A; ARG:195.A	TYR:62.A; TRP:58.A	___	___	___	___
		Camphene	___	TYR:62.A	LEU:162.A; LEU:165.A;	ARG:195.A; ASP:197,300.A; TRP:59.A; ALA:198.A	HIS:101.A; TYR:32.A; HIS:299.A; TRP:58.A	___	___	___	___
		Vertocitral	GLN:63.A	TYR:62.A	___	ASP:197,300.A; LEU:165.A; TRP:58.A	TRP:59.A; TYR:62.A; HIS:299.A	___	___	___	___
	GEO	Caryophyllene alcohol	GLY:351.A; GLN:302.A; ASN:301.A; ALA:310.A;THR:314.A;ARG:267.A	___	___	TRP:369.A; ASN:352.A;ASP:353.A; PHE:348.A; GLY:309.A; ILE:312.A; ARG:303.A	___	ASP:317.A; ASP:317.A	___	GLY:304.A	GLY:351.A;
		octanol	___	___	LEU:165.A; LEU:165.A	GLU:233.A;ARG:195.A; ASP:197,300.A; HIS:299.A; TRP:59.A;GLN:63.A	TYR:62.A	___	___	___	___
		Limonene	___	___	LEU:165.A;	ARG:195.A;ASP:197,300.A; TRP:58.A; GLN:63.A	TRP:59.A; TYR:62.A;	___	___	___	___
		Acarbose	THR:163.A,ASP:197.A, GLU233,240.A,LYS:200.A, HIS:305,201.A,TRP:59.A, GLN:63.A	___	ILE:235.A	HIS:101.A, LEU:162,165,237.A, ALA:198,307.A,TYR:62,151.A,TRP:58.A, ASP:300.A, GLU:60.A, GLY:306.A	___	___	___	LYS:200.A	___

Dalli et al. (2022), also reported effective *in silico* analysis of *Nigella sativa* essential oil bioactive compounds α-Phellandrene, β-Cymene, 4- Caranol, Thymol, α-Pinene, β-Pinene with α-amylase. Our findings were consistent with those reported by Ogunyemi et al. (2020), who cited *in vitro* and molecular docking investigations of phytochemicals (marsectohexol) derived from *Gongronema latifolium* as α-amylase inhibitors. Moreover, it validated the potential for the binding relationship between EOs and α-amylase, which was examined and verified by the use of the additional spectroscopic methods and fluorescence quenching technique documented in this work.

Binding interaction analysis between α-amylase enzyme and Eos

UV-VIS spectroscopy and florescent quenching are key techniques used to analyze changes in protein conformation upon its interaction with ligands (Wang et al., 2020). In the present study, the binding interaction of TEO, REO, and GEO with α-amylase was monitored.

UV-VIS spectral profile of native enzyme in the absence and presence of different volumes of EOs is displayed in Figure 3, it was observed that at 280 nm absorption intensity of α-amylase enzyme increased in the presence of EO's relative to control (free α-amylase).These data suggest a high likelihood of interaction between the protein and the inhibitor (EOs), even if the α-amylase's natural conformation was not significantly altered. The absorption peak(s) of a free protein and that of the protein-ligand complex are typically expected to differ when measured at the same wavelength range; this

http://www.jbb.uni-plovdiv.bg DOI: 10.69085/jbb20241001

difference may be explained by the protein's native structure changing as a result of its binding interaction with the ligand. Similar observations of increased absorbance of α-amylase enzyme in the presence of plant herbal extract have been reported in *Justicia carnea* extract (Anigboro et al., 2021).

The binding interaction of α-amylase enzyme with different EOs was further studied by fluorescence quenching assay. Earlier studies have suggested that phenylalanine, tyrosine, and tryptophan amino acids have been involved in the intrinsic endogenous fluorescent emission of enzymes (Zheng et al., 2020). The activity of the enzyme is therefore impacted by modifications to the microenvironments of these amino acid residues. By measuring the corresponding changes in the protein's maximum emission intrinsic fluorescence intensity, one may measure the ligand-protein interaction-induced modifications in the microenvironments of the enzyme's chromophoric groups (Wang et al., 2019; Zheng et al., 2020). In this study, we measured the α-amylase fluorescence emission intensities and evaluated the observed changes in the enzyme's intrinsic fluorescence at varying concentrations of EO's (50, 100, 150, 200, and 250µL) (Figure 4). The fluorescence emission spectra plots indicated that as the concentration of EOs increased, the intrinsic fluorescence intensity of α-amylase gradually decreased, indicating the presence of molecular interactions between α-amylase and EOs. These results were in consonance with the report given by Anigboro et al., (2021) where decreased intrinsic fluorescence of α-amylase enzyme was observed in the presence of plant herbal extract has been reported in *Justicia carnea* extract.

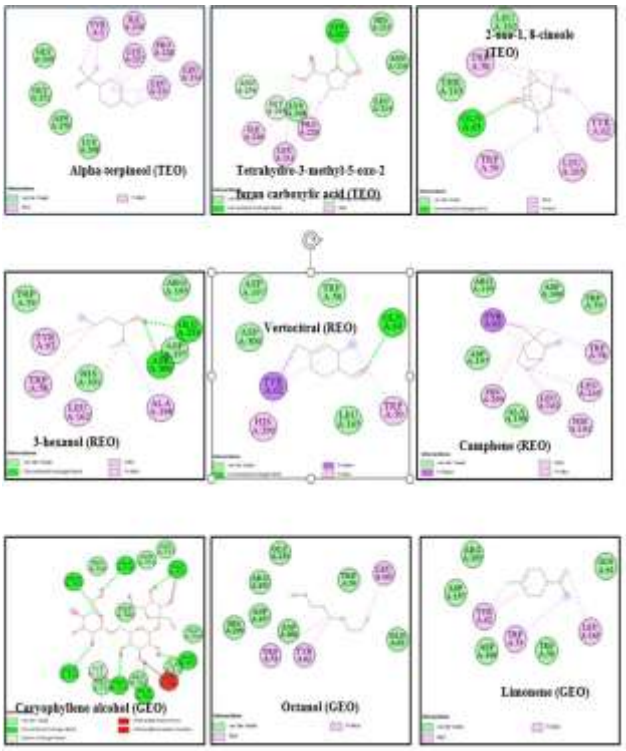

Figure 2. *2-D models of ligands with α-amylase*.

In vitro α-amylase inhibition

According to McCue et al. (2005), α-amylase inhibitory action is thought to slow down the metabolism of carbohydrates to manage blood sugar levels. One of the primary strategies used to reduce gastrointestinal glucose absorption is inhibiting α-amylase, an enzyme that breaks down carbohydrates.

Table 3. *Active site analysis of target enzymes*

Target enzyme	3-D model	Interacting Active site residues	Cavity	
			Area (SA) Å^2	Volume (SA) Å^3
α-amylase 3bai	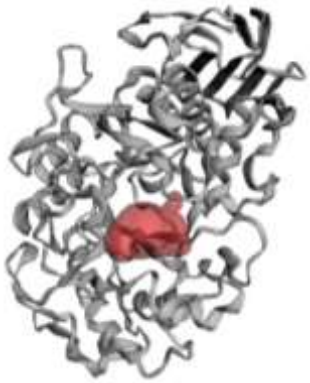	GLU:233.A,ASP:300.A, ARG:195.A LEU:1165.A ASP:197.A, HIS:299.A,GLN:63.A TYR:62,TRP:58,59.A HIS:101.A, LEU:162,165,237.A, ALA:198,307.A,TYR:62,151.A,TRP:58.A, ASP:300.A, GLU:60.A, GLY:306.A THR:163.A,ASP:197.A, GLU233,240.A,LYS:200.A, HIS:305,201.A,TRP:59.A, GLN:63.A GLU:233.A,ASP:300.A, HIS:101.A, LEU:162.A,GLN:63.A,ARG:195.A, ALA:198.A ASP:300,197.A, GLU:233.A, ALA:198.A, HIS:101.A HIS:101,299.A, TYR:62.A,TRP:58.A	239.626	225.493

http://www.jbb.uni-plovdiv.bg DOI: 10.69085/jbb20241001

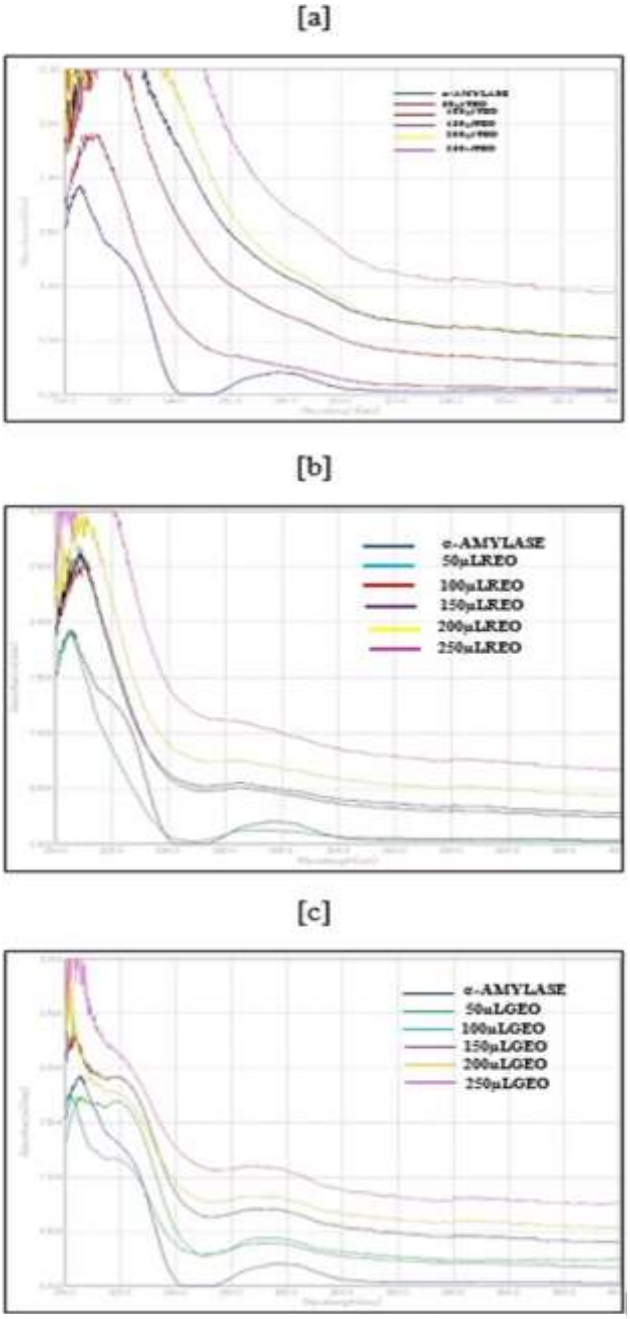

Figure 3 *UV-spectral analysis of TEO[a], REO[b], and GEO [c] showing interaction with α-amylase..*

This lowers the body's glucose levels, which helps to treat diabetes mellitus (McCue et al., 2005). Figure 5-7 provides evidence of the inhibitor's confirmed capacity to inhibit α-amylase.

As can be seen from Figure 5a, 6a, 7a, TEO, REO, and GEO all showed inhibition of α-amylase in a dose-dependent manner, exhibiting 26.29%, 85.41%, and 68.28% inhibition at 250µl (a higher volume used) in comparison to 69.39% inhibition at a concentration of 10µg/ml for acarbose, the standard inhibitor of α-amylase. For TEO, REO, and GEO, the 50% inhibition of α-amylase activity was reached at an IC-50 value of 34.9µg/ml, 486.4µg/ml, and 24.8µg/ml, respectively.

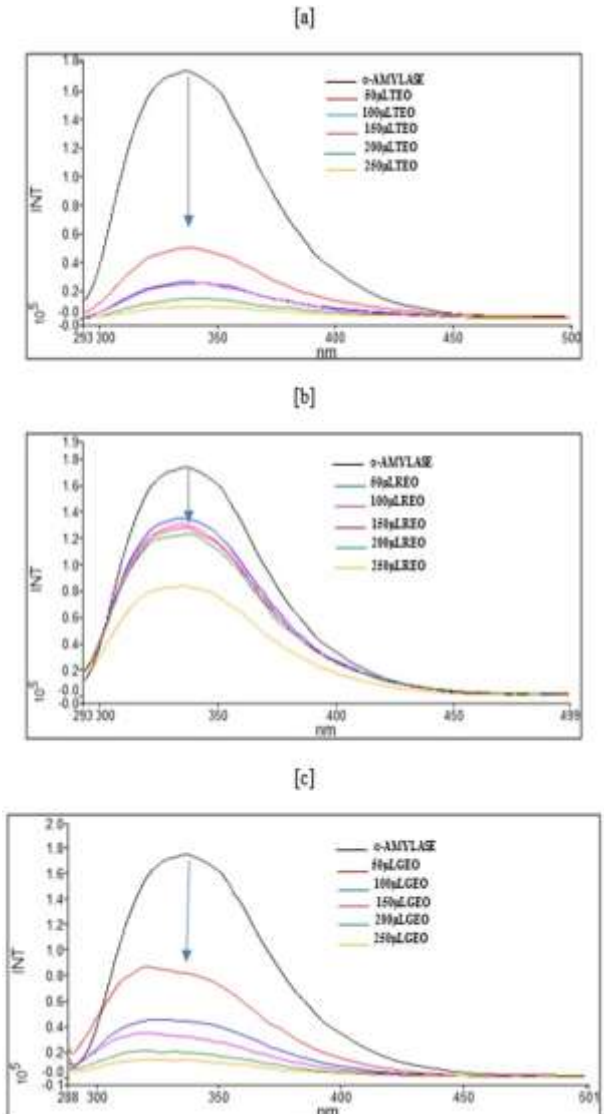

Figure 4. *Fluorescence Quenching analysis of TEO[a], REO[b], and GEO [c] showing interaction with α-amylase. Arrow indicates decreased INT.*

As shown in Figure 8, the positive control acarbose showed a lower IC-50 value of 3.79 µg/µl. In this study, the IC-50 values for α-amylase inhibition obtained from TEO (34.9µg/ml), REO (486.4µg/ml), and GEO (24.8µg/ml) were found to be lower than those obtained from *Sargassum angustifolium* phosphate buffer extract (1.85 mg/mL or 1850 µg mL-1) as reported by Nasab et al. 2020 and from *Justicia carnea* aqueous leaf extract (IC50 671.43 µg/mL), which was cited by Anigboro et al., 2021. The outcome showed that TEO, REO, and GEO inhibit α-amylase to a somewhat smaller extent than acarbose (IC50 = 3.79µg/µl). The hydrolases (enzyme class) are responsible for the metabolism of carbohydrates (complex or polysaccharides) by enzymes such as maltase, α-amylase, and α-glucosidase. After consuming

http://www.jbb.uni-plovdiv.bg DOI: 10.69085/jbb20241001

meals high in carbs, they produce glucose, or simple sugar, which causes blood sugar levels to rise immediately (Anigboro et al., 2018). Consequently, among other inhibitors interestingly, α-amylase inhibitors are extremely efficient in reducing impulsive blood sugar increases in type-II diabetics after they ingest meals rich in carbs (Ajiboye et al., 2019; Avwioroko et al., 2020). In this investigation, the relatively modest inhibitory potential of TEO, REO, and GEO as α-amylase inhibitors relative to acarbose is a beneficial characteristic. Previous research has also demonstrated that increased acarbose inhibition of α-amylase ultimately results in excessive starch hydrolysis retardation in the gastrointestinal tract (GI), which causes flatulence, discomfort, and pain in the abdomen in diabetics (Adefegha et al., 2015; Adefegha & Oboh, 2012).

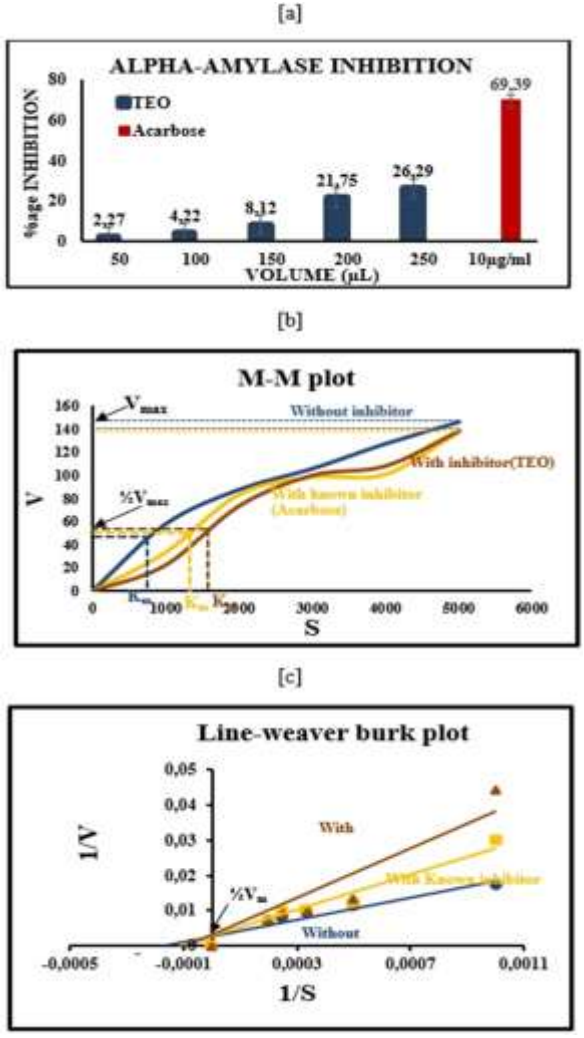

Figure 5. *α-amylase inhibition assay [a], Michaelis-Menten Plot [b], and Lineweaver-burk plot [c] showing inhibition of α-amylase activity by GEO.*

Our findings align with other research suggesting that unwarranted suppression of pancreatic α-amylase might result in aberrant bacterial fermentation of indigestible carbohydrates found in the colon (Apostolidis et al., 2007). As such, modest inhibition of α-amylase by TEO, REO, and GEO is suitable. Thus, it is believed that in diabetes individuals who can effectively ingest a meal heavy in sugar and carbs, the fairly limited potential of TEO, REO, and GEO to block α-amylase may prevent blood glucose levels from increasing dramatically. Due to the high α-amylase inhibitory capability of acarbose, it is inferred that TEO, REO, and GEO can establish minimally, or not-bit detrimental impacts.

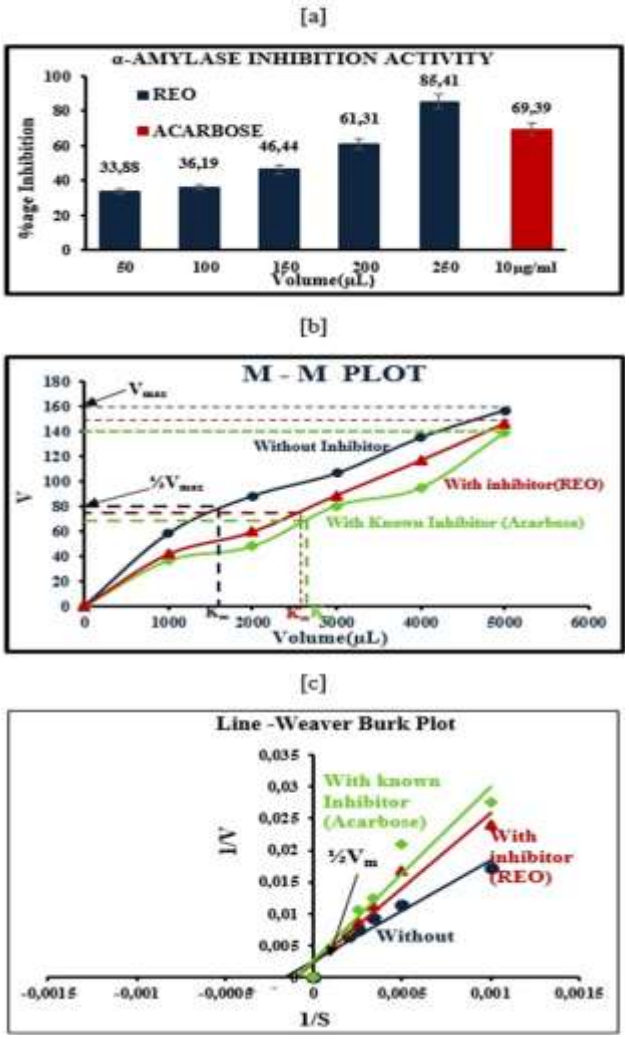

Figure 6. *α-amylase inhibition assay [a], Michaelis-Menten Plot [b], and Lineweaver-burk plot [c] showing inhibition of α-Amylase activity by REO.*

The mechanism of action of TEO, REO, and GEO on α-amylase was ascertained by an analysis of the Lineweaver-Burk and Michaelis-Menten plots, as illustrated in Figures 5b, c; 6b, c; 7b, c. The graphic illustrates how TEO, REO, and GEO competitively inhibited α-amylase. The maximal velocities (Vmax) remained unchanged when analyses of

TEO, REO, and GEO concentrations were conducted. Nevertheless, for these competitive inhibitors, the values for the Michaelis-Menten constant (Km) have increased (Figure 5b, c; 6b, c; 7b, c). The inhibitors (TEO, REO, and GEO) drive inhibition by competing with the substrate for the free enzyme's active site by generating an enzyme-inhibitor complex. It is postulated that the bio-active components present in the TEO, REO, and GEO bind to the active site of the α-amylase; by delaying the breakdown of oligosaccharides to disaccharides after competing with the substrate. The inhibition of α-amylase by the essential oil of *Laurus nobilis L*. was shown to occur through a competitive mechanism (Basak & Candan, 2013). Ahmed et al. (2020) also observed that alpha-amylase was competitively inhibited by the oils of *Allium cepa* (onion) and *Allium sativum* (garlic). Agnish and colleagues (2022) reported similar results with *Cymbopogon pendulus*, such as competitive suppression of α-amylase.

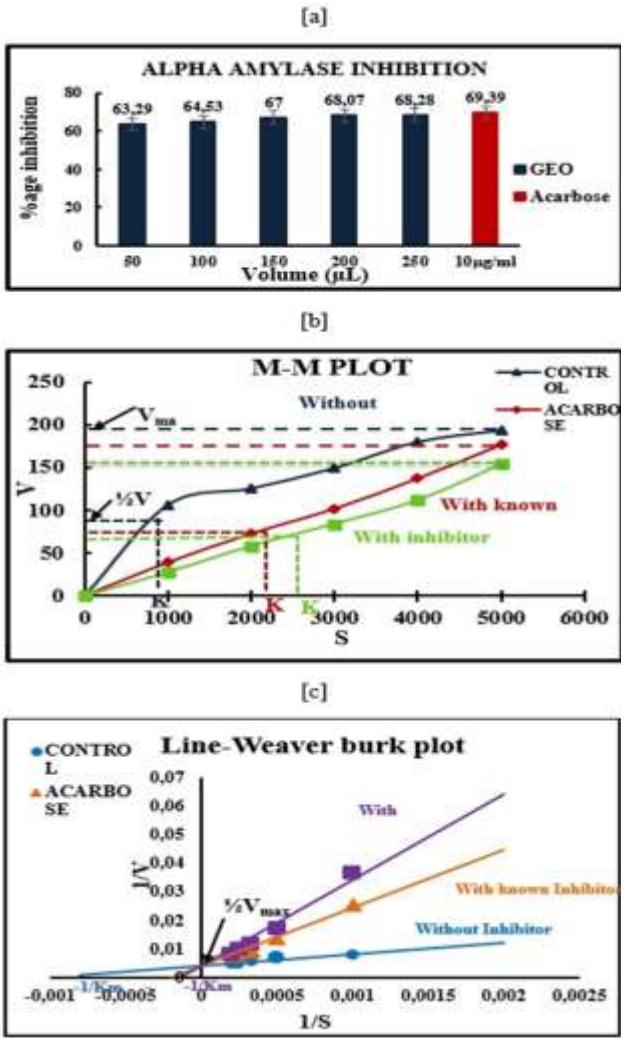

Figure 7. *α-amylase inhibition assay [a], Michaelis-Menten Plot [b], and Lineweaver-burk plot [c] showing inhibition of α-Amylase activity by GEO.*

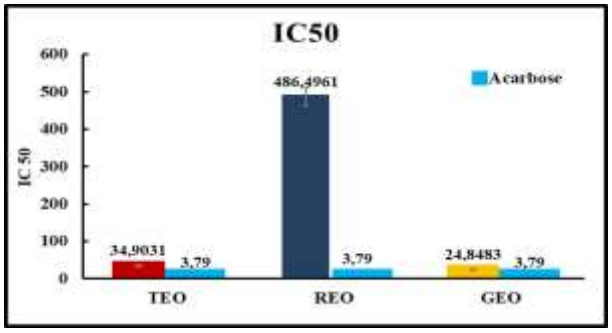

Figure 8. *IC50 of TEO, REO, GEO, and acarbose.*

The inhibitory efficacy of extracts from medicinal plants is mainly attributed to phytochemicals such as flavonoids, which are efficient in inhibiting α-amylase, according to research reported in the literature (Kazeem et al., 2013).

In vitro antioxidant assay

Earlier studies revealed that during D2TM, oxidative stress increased in the cells due to the accumulation of free reactive oxygen species thus enhancing diabetic complications (Asmat et al., 2016). It also seems that the generation of antioxidants reduces the risk of diabetes by mitigating free reactive oxygen species in the cells. Thus, the antioxidative effect of EOs viz: TEO, REO, and GEO on DPPH scavenging was also studied as shown in Figure 9. For instance: % DPPH scavenging activity at 50µl of TEO, REO, and GEO was 38%, 97%, and 60%, respectively. It was evident from the present results that EOs ameliorated oxidative stress which is corroborated by the earlier reports (Anigboro et al., 2021).

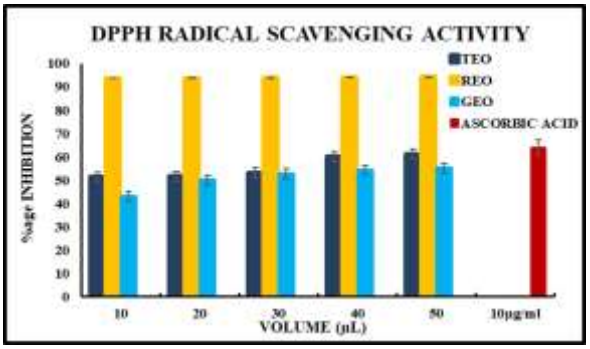

Figure 9. *DPPH radical scavenging activity of TEO, REO, and GEO.*

All in all, these investigations conclude that the inclusion of main and several minor bioactive components in-toto in TEO, REO, and GEO gives EOs strong antioxidant activity effects. The content, chemical structure, and degree of polymerization of antioxidants were shown to be correlated

with their antioxidant activity against DPPS and ABTS, as reported by Khan et al. (2020). Furthermore, high molecular weight phenolics, such as tannins, are more effective in scavenging free radicals. Additionally, Siddique et al. (2020) reported that *M. bracteata's* TEO scavenging activity varied from 35.3 to 89.2 ± 0.4%. Prior research by Viuda-Martos et al. (2010) revealed that oxygenated monoterpenes possibly monoterpenoid ketones might contribute most to REO's antioxidant potential of 38% scavenging activity. In another study, the antioxidant activity of *B. sacra* essential oil (GEO), based on the DPPH- scavenging activity, was found to be 57.50% (Rahmati-Joneidabad & Alizadehbehbahani, 2021). Studies have demonstrated that hyperglycemia both weakens the body's natural antioxidant defense mechanism and causes the production of reactive species (Derosa et al., 2020). On the other hand, it has also been shown that polyphenolic compounds and plant extracts have inhibitory effects against the production of advanced glycation end products and oxidative stress (Farombi et al., 2020; Khan et al., 2020). Because the phenolic-rich plant extract would be able to scavenge reactive species produced endogenously, thereby ameliorating oxidative stress-induced complications sometimes associated with diabetes mellitus, it follows that the high antioxidant potential expressed by EOs in the current study may provide an additional benefit to diabetic subjects who may use it for type 2 diabetes management (Derosa et al., 2020; Khan et al., 2020; Bejarano et al., 2019; Otuechere et al., 2020).

In silico ADMET properties

Drug characteristics such as absorption, distribution, metabolism, excretion, and toxicity (ADMET) and Prediction of Activity Spectra for Substances (PASS) are necessary for in vitro therapeutic applications (Wu et al., 2020). For all ligands used in molecular docking studies, including α-terpineol, Tetrahydro-3-methyl-5-oxo-2 furan carboxylic acid, 2-oxo-1,8-cineole (from TEO), 3-hexanol, Camphene, Vertocitral (from REO), Caryophyllene alcohol, octanol, Limonene (from GEO), and acarbose, the Lipinski Five Rule (RO5) finds drug similarity for all ligands. This criterion states that a ligand must have log P < 5, H-bond acceptors no. ≤ 10, number of H-bond donors ≤ 5, and 1vioation is permitted to have qualities comparable to medication. Every ligand complied with Weber, Egan, and Lipinski's guidelines. The ADMET characteristics and PASS analysis of all the phytochemicals were determined, including α-terpineol, Tetrahydro-3-methyl-5-oxo-2 furan carboxylic acid, 2-oxo-1,8-cineole (from TEO), 3-hexanol, Camphene, Vertocitral (from REO), Caryophyllene alcohol, octanol, Limonene (from GEO), and acarbose.

The oral activity of each ligand molecule is predicted by calculating other chemical parameters such as mlogP (partition coefficient) and TPSA (polar surface area), as indicated in Table 4. Except acarbose, all bioactive substances employed as ligands showed good concordance with RO5. All eight ligands were shown to be low molecular weight by ADMET and PASS analysis. According to reports, low-molecular-weight ligands are more likely than high-molecular-weight ligands to diffuse quickly and transfer across biological membranes (Srimai et al., 2013). Every ligand had a Log Po/w value that was within the permitted range. According to Abraham (2003), Log Po/w is a crucial characteristic in pharmacokinetic studies that assesses a drug's lipophilicity and the extent to which it diffuses in the human body after absorption. The total petroleum solvent (TPSA) values for α-terpineol (TEO), 3-hexanol (REO), and octanol (GEO) were 20.23 Å^2, vertocitral (derived from TEO) was 17.07 Å^2, 2-oxo-1,8-cineole was 26.30 Å^2, and Tetrahydro-3-methyl-5-oxo-2 furan carboxylic acid was 52.60 Å^2. Acarbose's TPSA was 321.17 Å^2. According to Wu et al. (2020), the Topological Polar Surface Area (TPSA) is a useful tool for interpreting drug transfer features, such as improved bioavailability, superior permeability, and exceptional intestine absorption. For drug molecules to harm the human body, they need to be significantly absorbed. The BBB invasion, bioavailability, good assimilation, and degree of drug absorption (including intestinal absorption) are all described by the TPSA value (Veber et al., 2002). Since it is clear from Table 4, the GI absorption (Gastrointestinal tract) of all the ligands was high excluding camphene from REO, caryophyllene alcohol and limonene from GEO, and acarbose. Likewise, all the ligands [α-terpineol, Tetrahydro-3-methyl-5-oxo-2 furan carboxylic acid, 2-oxo-1,8-cineole (from TEO), 3-hexanol, Camphene, Vertocitral (from REO), octanol, Limonene (from GEO)] were not substrate to P-gp (P-glycoprotein) efflux transporter excluding acarbose and caryophyllene alcohol from GEO. P-gp efflux carrier in the gut sends drugs back decreasing their absorption into the lumen (König et al., 2013). Bioactive substances such as α-terpineol, Tetrahydro-3-methyl-5-oxo-2 furan carboxylic acid, 2-oxo-1,8-cineole (from TEO), 3-hexanol, Camphene, Vertocitral (from REO), octanol, Limonene (from GEO), and acarbose possess non-inhibitory properties in contrast to the CYP450 enzyme series that is linked to the liver detoxification process in humans (Abraham, 2003; Srimai et al., 2013). The CYP2C9 enzyme was shown to be inhibited by camphene and limonene. Table 4 makes it clear that, except for acarbose, which deviates from these guidelines, all seven ligands satisfy the requirements of Lipinski, Veber, and Egan. These findings demonstrated that all ligands could readily interact with the target enzymes and could also be considered when determining the biological activity score.

RESEARCH ARTICLE

Table 4. *ADMET properties of bioactive compounds used as ligands.*

	TEO			REO			GEO			
	α-terpineol	Tetrahydro-3-methyl-5-oxo-2 furan carboxylic acid	2-oxo-1,8-cineole	3-hexanol	Camphene	Vertocitral	Caryophyllene alcohol	octanol	Limonene	**Acarbose**
Physiochemical Properties										
Formula	**$C_{10}H_{18}O$**	**$C_7H_{10}O_4$**	**$C_{10}H_{16}O_2$**	**$C_6H_{14}O$**	**$C_{10}H_{16}$**	**$C_9H_{14}O$**	**$C_{18}H_{32}O_{16}$**	**$C_8H_{18}O$**	**$C_{10}H_{16}$**	**$C_{25}H_{43}NO_{18}$**
Molecular weight	154.25 g/mol	158.15 g/mol	168.23 g/mol	102.17 g/mol	136.23 g/mol	138.21 g/mol	504.44 g/mol	130.23 g/mol	136.23 g/mol	645.60 g/mol
Num. heavy atoms	11	11	12	7	10	10	34	9	10	44
Num. arom. heavy atoms	0	0	0	0	0	0	0	0	0	0
Fraction Csp3	0.80	0.71	0.90	1.00	0.80	0.67	1.00	1.00	0.60	0.92
Num. rotatable bonds	1	2	0	3	0	1	8	6	1	9
Num. H-bond acceptors	1	4	2	1	0	1	16	1	0	19
Num. H-bond donors	1	0	0	1	0	0	11	1	0	14
Molecular Refractivity	48.80	36.22	47.32	32.12	45.22	42.99	100.54	41.73	47.12	136.69
TPSA	20.23 Å²	52.60 Å²	26.30 Å²	20.23 Å²	0.00 Å²	17.07 Å²	268.68 Å²	20.23 Å²	0.00 Å²	321.17 Å²
Lipophilicity										
Log $P_{o/w}$ (iLOGP)	2.51	1.51	2.15	2.14	2.58	2.00	0.00	2.51	2.72	0.63
Log $P_{o/w}$ (XLOGP3)	3.39	0.57	1.22	1.65	4.22	1.45	-5.85	3.00	4.57	-8.53
Log $P_{o/w}$ (WLOGP)	2.50	0.11	1.92	1.56	3.00	2.18	-7.57	2.34	3.31	-8.56
Log $P_{o/w}$ (MLOGP)	2.30	0.21	1.38	1.53	4.29	1.89	-6.15	2.22	3.27	-6.94
Log $P_{o/w}$ (SILICOS-IT)	2.17	0.69	2.52	1.11	3.08	2.18	-5.93	2.14	2.97	-7.69
Consensus Log $P_{o/w}$	2.58	0.62	1.84	1.60	3.43	1.94	-5.10	2.44	3.37	-6.22
Water Solubility										
Log *S* (ESOL)	-2.87	-1.05	-1.65	-1.31	-3.34	-1.54	1.25	-2.14	-3.50	2.13
Solubility	2.10e-01 mg/ml; 1.36e-03 mol/l	1.42e+01 mg/ml; 8.96e-02 mol/l	3.75e+00 mg/ml; 2.23e-02 mol/l	4.95e+00 mg/ml; 4.84e-02 mol/l	6.18e-02 mg/ml; 4.54e-04 mol/l	3.95e+00 mg/ml; 2.86e-02 mol/l	8.89e+03 mg/ml; 1.76e+01 mol/l	9.40e-01 mg/ml; 7.22e-03 mol/l	4.33e-02 mg/ml; 3.18e-04 mol/l	8.61e+04 mg/ml; 1.33e+02 mol/l
Class	Soluble	Very soluble	Very soluble	Very soluble	Soluble	Very soluble	Highly soluble	Soluble	Soluble	Highly soluble
Log *S* (Ali)	-3.49	-1.25	-1.37	-1.69	-3.93	-1.41	0.88	-3.09	-4.29	2.56
Solubility	4.95e-02 mg/ml; 3.21e-04 mol/l	8.95e+00 mg/ml; 5.66e-02 mol/l	7.18e+00 mg/ml; 4.27e-02 mol/l	2.09e+00 mg/ml; 2.05e-02 mol/l	1.60e-02 mg/ml; 1.17e-04 mol/l	5.32e+00 mg/ml; 3.85e-02 mol/l	3.80e+03 mg/ml; 7.53e+00 mol/l	1.06e-01 mg/ml; 8.14e-04 mol/l	6.93e-03 mg/ml; 5.09e-05 mol/l	2.32e+05 mg/ml; 3.60e+02 mol/l
Class	Soluble	Very soluble	Very soluble	Very soluble	Soluble	Very soluble	Highly soluble	Soluble	Moderately soluble	Highly soluble
Log *S* (SILICOS IT)	-1.69	-0.61	-2.35	-1.27	-2.48	-1.53	5.43	-2.49	-2.26	6.40
Solubility	3.17e+00 mg/ml ; 2.06e-02 mol/l	3.90e+01 mg/ml ; 2.47e-01 mol/l	7.51e-01 mg/ml ; 4.47e-03 mol/l	5.53e+00 mg/ml ; 5.41e-02 mol/l	4.55e-01 mg/ml ; 3.34e-03 mol/l	4.07e+00 mg/ml; 2.94e-02 mol/l	1.35e+08 mg/ml ; 2.68e+05 mol/l	4.23e-01 mg/ml; 3.25e-03 mol/l	7.54e-01 mg/ml; 5.53e-03 mol/l	1.62e+09 mg/ml ; 2.51e+06 mol/l
Class	Soluble	Soluble	Soluble	Soluble	Soluble	Soluble	Soluble	Soluble	Soluble	Soluble
Pharmacokinetics										
GI absorption	High	High	High	High	Low	High	Low	High	Low	
BBB permeant	Yes	No	Yes	Yes	Yes	Yes	No	Yes	Yes	No
P-gp substrate	No	No	No	No	No	No	Yes	No	No	Yes
CYP1A2 inhibitor	No	No	No	No	No	No	No	No	No	No
CYP2C19 inhibitor	No	No	No	No	No	No	No	No	No	No
CYP2C9 inhibitor	No	No	No	No	Yes	No	No	No	Yes	No
CYP2D6 inhibitor	No	No	No	No	No	No	No	No	No	No
CYP3A4 inhibitor	No	No	No	No	No	No	No	No	No	No
LogK_p (skin permeation)	-4.83 cm/s	-6.86 cm/s	-6.46 cm/s	-5.75 cm/s	-4.13 cm/s	-6.11 cm/s	-13.53 cm/s	-4.96 cm/s	-3.89 cm/s	-16.29 cm/s
Druglikeness										
Lipinski	Yes; 0 violation	Yes; 0 violation	Yes; 0 violation	Yes; 0 violation	Yes; 1 violation: MLOGP>4.15	Yes; 0 violation	No; 3 violations: MW>500, NorO>10, NHorOH>5	Yes; 0 violation	Yes; 0 violation	No; 3 violations: MW>500, NorO>10, NHorOH>5
Ghose	No; 1 violation: MW<160	No; 2 violations: MW<160, MR<40	Yes	No; 2 violations: MW<160, MR<40	No; 1 violation: MW<160	No; 1 violation: MW<160	No; 2 violations: MW>480, WLOGP<-0.4	No; 1 violation: MW<160	No; 1 violation: MW<160	No; 4 violations: MW>480, WLOGP<-0.4, MR>130, #atoms>70
Veber	Yes	Yes	Yes	Yes	Yes	Yes	No; 1 violation: TPSA>140	Yes	Yes	No; 1 violation: TPSA>140
Egan	Yes	Yes	Yes	Yes	Yes	Yes	No; 1 violation: TPSA>131.6	Yes	Yes	No; 1 violation: TPSA>131.6

http://www.jbb.uni-plovdiv.bg DOI: 10.69085/jbb20241001

Table 4. *ADMET properties of bioactive compounds used as ligands (continue)*

	TEO			REO			GEO			
	α-terpineol	Tetrahydro-3-methyl-5-oxo-2 furan carboxylic acid	2-oxo-1,8-cineole	3-hexanol	Camphene	Vertocitral	Caryophyllene alcohol	octanol	Limonene	**Acarbose**
Muegge	No; 2 violations: MW<200, Heteroatoms<2	No; 1 violation: MW<200	No; 1 violation: MW<200	No; 2 violations: MW<200, Heteroatoms<2	No; 2 violations: MW<200, Heteroatoms<2	No; 2 violations: MW<200, Heteroatoms<2	No; 4 violations: XLOGP3<-2, TPSA>150, H-acc>10, H-don>5	No; 2 violations: MW<200, Heteroatoms<2	No; 2 violations: MW<200, Heteroatoms<2	No; 5 violations: MW>600, XLOGP3<-2, TPSA>150, H-acc>10, H-don>5
Bioavailability Score	0.55	0.55	0.55	0.55	0.55	0.55	0.17	0.55	0.55	0.17
Medicinal Chemistry										
PAINS	0 alert	0 alert	0 alert	0 alert	0 alert	0 alert	0 alert	0 alert	0 alert	0 alert
Brenk	1 alert: isolated alkene	1 alert: more_than_2_esters	0 alert	0 alert	1 alert: isolated alkene	2 alerts: aldehyde, isolated alkene	0 alert	0 alert	1 alert: isolated alkene	1 alert: isolated alkene
Leadlikeness	No; 1 violation: MW<250	No; 1 violation: MW<250	No; 1 violation: MW<250	No; 1 violation: MW<250	No; 2 violations: MW<250, XLOGP3>3.5	No; 1 violation: MW<250	No; 2 violations: MW>350, Rotors>7	No; 1 violation: MW<250	No; 2 violations: MW<250, XLOGP3>3.5	No; 2 violations: MW>350, Rotors>7
Synthetic accessibility	3.24	2.84	3.69	1.25	3.50	3.49	6.28	1.44	3.46	7.

To evaluate the biological activity analysis of isolated ligands further, the structure-based PASS Online biological activity prediction tool was employed. It generates Pa and Pi values between 0.000 and 1.000. If the probable activity (Pa) value of the chemical is greater than the likely inactivity (Pi), the substance is said to have pharmacological potential. Table 5 illustrates the expected significant anti-diabetic, antioxidant, and anticancer activities, and many other biological activities of each ligand. Pharmacological action may indicate the discovery of a novel chemical (Goel et al., 2011; Khurana et al., 2011). Given the predicted Pa values in this instance, the discovered bioactive molecules may be novel important molecules for the treatment of T2DM. They also imply that the compounds have a wide range of pharmacological biological activities and might be targeted against certain receptors. The strong biological activity of the isolated compounds, including their ability to scavenge ROS and fight diseases, is shown by their Pa value. Reza et al., (2021), observed comparable results in their examination of the antiproliferative and antioxidant characteristics of the bioactive edible vegetable fraction of *Achyranthes ferruginea* Roxb.

Conclusion

A distinguished threat has emerged worldwide currently; due to the adverse side effects of anti-diabetic drugs on human health. To combat this problem, medicinal plant-derived drugs with increased potency and less detrimental side effects than presently used pharmaceuticals are being researched. This analysis aimed to investigate the phytochemicals in essential oil derived from *Melaleuca alternifolia, Rosmarinus officinalis, Boswellia serrata* essential oil that could be used to inhibit carbohydrate-digesting enzymes. The successful docking of every ligand with the target α-amylase enzyme has been verified by molecular docking and *in vitro* experiments. The participation of phytochemicals such as flavonoids, saponins, and tannins may have significantly contributed to the inhibitory action of the TEO, REO, and GEO, which demonstrated the best inhibitory effect on the two enzymes under study. Therefore, we suggest that *Melaleuca alternifolia*, *Rosmarinus officinalis, Boswellia serrata* essential oil, which may be found in herbal medications and may represent prospective treatment options, may serve as an inhibitor of carbohydrate-digesting enzymes. However, in order to open the way for these compounds in drug development, various research should be carried out to determine these compounds utilizing *in vitro* and *in vitro* models.

Table 5. *Bioactivity score of all the ligands.*

Ligand Name	Activity	Pa	Pi
α-terpineol (TEO)	Respiratory analeptic	0.862	0.005
	Carminative	0.837	0.003
	CYP2C12 substrate	0.853	0.023
	Antieczematic	0.825	0.014
	Analeptic	0.804	0.005
	Testosterone 17beta-dehydrogenase (NADP+) inhibitor	0.814	0.022
	CYP2J substrate	0.808	0.019
	Alkenylglycerophosphocholine hydrolase inhibitor	0.763	0.023
	Alkylacetylglycerophosphatase inhibitor	0.753	0.014
	Ubiquinol-cytochrome-c reductase inhibitor	0.775	0.041
	Glutamyl endopeptidase II inhibitor	0.744	0.018
	Phosphatidylcholine-retinol O-acyltransferase inhibitor	0.727	0.012
	Acylcarnitine hydrolase inhibitor	0.733	0.022
	Adenomatous polyposis treatment	0.710	0.007
	Aspulvinone dimethylallyltransferase inhibitor	0.750	0.048
	Fibrinolytic	0.718	0.017
	5-O-(4-coumaroyl)-D-quinate 3'-monooxygenase inhibitor	0.717	0.020
Tetrahydro-3-methyl-5-oxo-2-furan carboxylic acid (TEO)	Ubiquinol-cytochrome-c reductase inhibitor	0.934	0.003
	CYP2H substrate	0.923	0.005
	HIF1A expression inhibitor	0.793	0.012
	Antieczematic	0.798	0.019
	Chymosin inhibitor	0.797	0.021
	Acrocylindropepsin inhibitor	0.797	0.021
	Saccharopepsin inhibitor	0.797	0.021
	General pump inhibitor	0.773	0.004
	H+-exporting ATPase inhibitor	0.749	0.003
	H+-transporting two-sector ATPase inhibitor	0.747	0.004
	Phosphatase inhibitor	0.748	0.006
	Testosterone 17beta-dehydrogenase (NADP+) inhibitor	0.743	0.041
	Lipid metabolism regulator	0.711	0.010
	Antimetastatic	0.703	0.002
	Aspulvinone dimethylallyltransferase inhibitor	0.707	0.061
2-oxo-1,8-cineole (TEO)	Respiratory analeptic	0.863	0.005
	CYP2C12 substrate	0.875	0.018
	Alcohol dehydrogenase substrate	0.832	0.001
	Testosterone 17beta-dehydrogenase (NADP+) inhibitor	0.843	0.016
	Analeptic	0.785	0.006
	Antiseborrheic	0.765	0.026
	Antiprotozoal	0.737	0.004
	CYP2J substrate	0.763	0.031
	CYP2B5 substrate	0.708	0.009
	Acylcarnitine hydrolase inhibitor	0.718	0.024
	CYP2J2 substrate	0.716	0.029
	Membrane permeability inhibitor	0.705	0.037
	Phobic disorders treatment	0.722	0.066
	Aspulvinone dimethylallyltransferase inhibitor	0.705	0.062
3-hexanol (REO)	Alkylacetylglycerophosphatase inhibitor	0.944	0.002
	5 Hydroxytryptamine release stimulant	0.943	0.003
	Chymosin inhibitor	0.942	0.003
	Acrocylindropepsin inhibitor	0.942	0.003
	Saccharopepsin inhibitor	0.942	0.003
	Sphinganine kinase inhibitor	0.936	0.003
	Sugar-phosphatase inhibitor	0.930	0.003
	Acylcarnitine hydrolase inhibitor	0.929	0.003
	Polyporopepsin inhibitor	0.921	0.004

http://www.jbb.uni-plovdiv.bg DOI: 10.69085/jbb20241001

Xylan endo-1.3-beta-xylosidase inhibitor	0.917	0.002
Beta-mannosidase inhibitor	0.910	0.002
Ubiquinol-cytochrome-c reductase inhibitor	0.912	0.004
CYP2C12 substrate	0.914	0.009
Alcohol oxidase inhibitor	0.906	0.002
Acetylesterase inhibitor	0.904	0.003
Prostaglandin-A1 DELTA-isomerase inhibitor	0.903	0.002
Pro-opiomelanocortin converting enzyme inhibitor	0.905	0.004
Fucosterol-epoxide lyase inhibitor	0.902	0.003
Alkenylglycerophosphocholine hydrolase inhibitor	0.900	0.005
Macrophage colony stimulating factor agonist	0.896	0.002
Sarcosine oxidase inhibitor	0.893	0.003
Glucan 1.4-alpha-maltotriohydrolase inhibitor	0.890	0.002
Carboxypeptidase Taq inhibitor	0.887	0.003
Testosterone 17beta-dehydrogenase (NADP+) inhibitor	0.891	0.008
CYP2J substrate	0.888	0.005
GST A substrate	0.883	0.004
Pullulanase inhibitor	0.883	0.004
IgA-specific serine endopeptidase inhibitor	0.880	0.003
Fragilysin inhibitor	0.878	0.004
Glutamyl endopeptidase II inhibitor	0.878	0.004
CYP2J2 substrate	0.877	0.005
BRAF expression inhibitor	0.874	0.001
Cutinase inhibitor	0.873	0.003
Membrane integrity agonist	0.883	0.015
Feruloyl esterase inhibitor	0.871	0.005
NADPH-cytochrome-c2 reductase inhibitor	0.741	0.012
Pseudolysin inhibitor	0.741	0.013
Carnitinamidase inhibitor	0.733	0.006
Aspartate-ammonia ligase inhibitor	0.731	0.006
Alkenylglycerophosphoethanolamine hydrolase inhibitor	0.728	0.005
Transketolase inhibitor	0.727	0.004
Peroxidase inhibitor	0.731	0.009
Alpha-N-acetylgalactosaminidase inhibitor	0.723	0.001
Biotinidase inhibitor	0.724	0.005
D-lactate dehydrogenase (cytochrome) inhibitor	0.720	0.002
Mycothiol-S-conjugate amidase inhibitor	0.722	0.004
N-formylmethionyl-peptidase inhibitor	0.720	0.005
Pterin deaminase inhibitor	0.722	0.009
Aryldialkylphosphatase inhibitor	0.716	0.004
Superoxide dismutase inhibitor	0.722	0.012
Mannan endo-1.6-alpha-mannosidase inhibitor	0.711	0.003
D-lactate-2-sulfatase inhibitor	0.709	0.001
Formaldehyde transketolase inhibitor	0.715	0.009
Phosphatidylserine decarboxylase inhibitor	0.716	0.010
GABA aminotransferase inhibitor	0.710	0.004
Long-chain-aldehyde dehydrogenase inhibitor	0.710	0.005
Aminoacylase inhibitor	0.707	0.004
Lysostaphin inhibitor	0.711	0.008
Polygalacturonase inhibitor	0.706	0.004
MMP9 expression inhibitor	0.706	0.006
Peptide-tryptophan 2.3-dioxygenase inhibitor	0.704	0.004
Choline-phosphate cytidylyltransferase inhibitor	0.704	0.005
Creatininase inhibitor	0.710	0.012
Hydroxylamine oxidase inhibitor	0.702	0.004
Adenomatous polyposis treatment	0.704	0.007

http://www.jbb.uni-plovdiv.bg DOI: 10.69085/jbb20241001

	Methylumbelliferyl-acetate deacetylase inhibitor	0.705	0.008
	Glutathione thiolesterase inhibitor	0.713	0.016
	D-xylulose reductase inhibitor	0.701	0.005
	Protein-disulfide reductase (glutathione) inhibitor	0.713	0.019
	Fibrinolytic	0.704	0.021
	Mucomembranous protector	0.724	0.046
	Antieczematic	0.706	0.044
Vertocitral (REO)	Antieczematic	0.893	0.005
	Ubiquinol-cytochrome-c reductase inhibitor	0.807	0.031
	Phosphatase inhibitor	0.774	0.004
	CYP2J substrate	0.787	0.024
	CDP-glycerol glycerophosphotransferase inhibitor	0.787	0.033
	Carminative	0.753	0.005
	Testosterone 17beta-dehydrogenase (NADP+) inhibitor	0.759	0.037
	CYP2C12 substrate	0.735	0.051
Camphene (REO)	Antieczematic	0.882	0.006
	Testosterone 17beta-dehydrogenase (NADP+) inhibitor	0.873	0.010
	CYP2J substrate	0.829	0.014
	Cardiovascular analeptic	0.816	0.004
	Acylcarnitine hydrolase inhibitor	0.779	0.016
	5-O-(4-coumaroyl)-D-quinate 3'-monooxygenase inhibitor	0.762	0.012
	Phobic disorders treatment	0.782	0.040
	Alkylacetylglycerophosphatase inhibitor	0.738	0.015
	Dermatologic	0.726	0.006
	CYP2J2 substrate	0.738	0.024
	Alkenylglycerophosphocholine hydrolase inhibitor	0.737	0.027
	Phosphatase inhibitor	0.710	0.011
	Aspulvinone dimethylallyltransferase inhibitor	0.746	0.049
Caryophyllene alcohol (GEO)	Fructan beta-fructosidase inhibitor	0.986	0.000
	Exoribonuclease II inhibitor	0.986	0.000
	Beta-glucosidase inhibitor	0.986	0.000
	Fucosterol-epoxide lyase inhibitor	0.984	0.001
	Levanase inhibitor	0.984	0.001
	Levansucrase inhibitor	0.982	0.000
	Sucrose alpha-glucosidase inhibitor	0.968	0.000
	Polyribonucleotide nucleotidyltransferase inhibitor	0.966	0.000
	Beta galactosidase inhibitor	0.963	0.000
	Sugar-phosphatase inhibitor	0.963	0.002
	Respiratory analeptic	0.960	0.003
	Beta-fructofuranosidase inhibitor	0.957	0.000
	Alkenylglycerophosphocholine hydrolase inhibitor	0.957	0.002
	CDP-glycerol glycerophosphotransferase inhibitor	0.954	0.003
	Benzoate-CoA ligase inhibitor	0.951	0.002
	Sweetener	0.944	0.000
	Sucrose-phosphate synthase inhibitor	0.937	0.000
	Glycerol dehydrogenase inhibitor	0.897	0.001
	Analeptic	0.896	0.003
	Beta-adrenergic receptor kinase inhibitor	0.897	0.005
	G-protein-coupled receptor kinase inhibitor	0.897	0.005
	Alpha.alpha-trehalase inhibitor	0.890	0.001
	Beta-D-fucosidase inhibitor	0.889	0.001
	Cyclomaltodextrin glucanotransferase inhibitor	0.888	0.000
	Mycothiol-S-conjugate amidase inhibitor	0.889	0.002
	Lactase inhibitor	0.889	0.002
	Sucrose phosphorylase inhibitor	0.880	0.000
	Vasoprotector	0.882	0.003
	Membrane permeability inhibitor	0.878	0.004

http://www.jbb.uni-plovdiv.bg DOI: 10.69085/jbb20241001

	3-Phytase inhibitor	0.868	0.003
	Alkenylglycerophosphoethanolamine hydrolase inhibitor	0.863	0.002
	Membrane integrity agonist	0.875	0.017
	Beta-N-acetylhexosaminidase inhibitor	0.857	0.000
	Beta-amylase inhibitor	0.854	0.001
	Glucan 1.3-alpha-glucosidase inhibitor	0.853	0.001
	Lactose synthase inhibitor	0.854	0.002
	Histamine release stimulant	0.748	0.003
	Galactolipase inhibitor	0.745	0.004
	Mannosyl-glycoprotein endo-beta-N-acetylglucosaminidase inhibitor	0.742	0.002
	Protein-tyrosine sulfotransferase inhibitor	0.740	0.004
	Ketohexokinase inhibitor	0.737	0.001
	Sucrose-phosphate phosphatase inhibitor	0.735	0.000
	Antidiabetic	0.739	0.005
	NAD(P)+-arginine ADP-ribosyltransferase inhibitor	0.743	0.009
	Glucan 1.4-beta-glucosidase inhibitor	0.735	0.002
	Glycosylceramidase inhibitor	0.734	0.002
	H+-exporting ATPase inhibitor	0.732	0.004
	Antihypoxic	0.731	0.005
	Chitinase inhibitor	0.729	0.004
	Endo-1.4-beta-xylanase inhibitor	0.727	0.002
	Amylosucrase inhibitor	0.724	0.000
	Oligo-1.6-glucosidase inhibitor	0.725	0.001
	GABA aminotransferase inhibitor	0.727	0.004
	Alpha-amylase inhibitor	0.724	0.002
	Antiviral (Influenza)	0.724	0.004
	Isoamylase inhibitor	0.748	0.003
	Xylose isomerase inhibitor	0.745	0.004
	Interleukin 2 agonist	0.742	0.002
	Fructose-2.6-bisphosphate 6-phosphatase inhibitor	0.740	0.004
	Mannotetraose 2-alpha-N-acetylglucosaminyltransferase inhibitor	0.737	0.001
	4-Nitrophenylphosphatase inhibitor	0.735	0.000
	Lipotropic	0.739	0.005
	Alpha.alpha-trehalose phosphorylase inhibitor	0.743	0.009
	Alpha-L-rhamnosidase inhibitor	0.735	0.002
	Undecaprenyldiphospho-muramoylpentapeptide beta-N-acetylglucosaminyltransferase inhibitor	0.734	0.002
	Wound healing agent	0.732	0.004
	[phosphorylase] phosphatase inhibitor	0.731	0.005
	Immunosuppressant	0.729	0.004
Octanol (GEO)	Sugar-phosphatase inhibitor	0.965	0.002
	Alkenylglycerophosphocholine hydrolase inhibitor	0.958	0.002
	Carboxypeptidase Taq inhibitor	0.952	0.001
	Alkylacetylglycerophosphatase inhibitor	0.951	0.002
	Glucan 1.4-alpha-maltotriohydrolase inhibitor	0.942	0.001
	Dextranase inhibitor	0.943	0.002
	Fucosterol-epoxide lyase inhibitor	0.940	0.002
	Pullulanase inhibitor	0.940	0.002
	Gluconate 5-dehydrogenase inhibitor	0.939	0.001
	Peptide-N4-(N-acetyl-beta-glucosaminyl)asparagine amidase inhibitor	0.938	0.001
	Ubiquinol-cytochrome-c reductase inhibitor	0.937	0.003
	Polyporopepsin inhibitor	0.936	0.003
	Sphinganine kinase inhibitor	0.933	0.003
	Exoribonuclease II inhibitor	0.930	0.002
	Alkanal monooxygenase (FMN-linked) inhibitor	0.929	0.002
	Levanase inhibitor	0.929	0.002

http://www.jbb.uni-plovdiv.bg DOI: 10.69085/jbb20241001

	Poly(alpha-L-guluronate) lyase inhibitor	0.928	0.002
	Xylan endo-1.3-beta-xylosidase inhibitor	0.927	0.002
	Poly(beta-D-mannuronate) lyase inhibitor	0.923	0.001
	Saccharopepsin inhibitor	0.925	0.004
	Acrocylindropepsin inhibitor	0.925	0.004
	Chymosin inhibitor	0.925	0.004
	Phobic disorders treatment	0.925	0.004
	Cutinase inhibitor	0.897	0.003
	Superoxide dismutase inhibitor	0.897	0.004
	Prenyl-diphosphatase inhibitor	0.889	0.002
	CYP2J substrate	0.892	0.005
	Procollagen N-endopeptidase inhibitor	0.885	0.002
	Glucan endo-1.3-beta-D-glucosidase inhibitor	0.886	0.003
	Rhamnulose-1-phosphate aldolase inhibitor	0.880	0.002
	CYP2J2 substrate	0.881	0.004
	Sclerosant	0.876	0.001
	Steroid N-acetylglucosaminyltransferase inhibitor	0.874	0.002
	GST A substrate	0.876	0.004
	Leukopoiesis stimulant	0.873	0.002
	G-protein-coupled receptor kinase inhibitor	0.875	0.006
	Beta-adrenergic receptor kinase inhibitor	0.875	0.006
	Arginine 2-monooxygenase inhibitor	0.872	0.004
	Trimethylamine-oxide aldolase inhibitor	0.869	0.002
	N-acetylneuraminate 7-O(or 9-O)-acetyltransferase inhibitor	0.866	0.004
	Alkenylglycerophosphoethanolamine hydrolase inhibitor	0.865	0.002
	Testosterone 17beta-dehydrogenase (NADP+) inhibitor	0.871	0.011
	All-trans-retinyl-palmitate hydrolase inhibitor	0.862	0.003
	5-O-(4-coumaroyl)-D-quinate 3'-monooxygenase inhibitor	0.863	0.004
Octanol (GEO)	Pro-opiomelanocortin converting enzyme inhibitor	0.866	0.007
	Membrane integrity agonist	0.874	0.018
	D-lactaldehyde dehydrogenase inhibitor	0.859	0.003
	Reductant	0.731	0.005
	Centromere associated protein inhibitor	0.732	0.006
	Alkylglycerone-phosphate synthase inhibitor	0.730	0.005
	Styrene-oxide isomerase inhibitor	0.729	0.003
	Aspartate-ammonia ligase inhibitor	0.731	0.006
	Endoglycosylceramidase inhibitor	0.722	0.002
	Mucositis treatment	0.739	0.019
	Catechol 2.3-dioxygenase inhibitor	0.721	0.003
	Beta-D-fucosidase inhibitor	0.719	0.002
	Phosphatidylinositol diacylglycerol-lyase inhibitor	0.720	0.003
	Coenzyme-B sulfoethylthiotransferase inhibitor	0.718	0.002
	N-formylmethionyl-peptidase inhibitor	0.720	0.005
	Pectin lyase inhibitor	0.716	0.003
	Glycine dehydrogenase (decarboxylating) inhibitor	0.716	0.004
	Glycopeptide alpha-N-acetylgalactosaminidase inhibitor	0.715	0.004
	Acylaminoacyl-peptidase inhibitor	0.714	0.004
	Plastoquinol-plastocyanin reductase inhibitor	0.713	0.003
	Omptin inhibitor	0.726	0.017
	ADP-thymidine kinase inhibitor	0.721	0.012
	CYP4A substrate	0.710	0.003
	Aryldialkylphosphatase inhibitor	0.712	0.004
	L-glucuronate reductase inhibitor	0.712	0.006
	Glucan 1.4-beta-glucosidase inhibitor	0.708	0.002
	Anesthetic general	0.712	0.006
	Limulus clotting factor B inhibitor	0.717	0.011
	Polygalacturonase inhibitor	0.709	0.004

Octanol (GEO)	Peptidoglycan glycosyltransferase inhibitor	0.707	0.004
	Gastrin inhibitor	0.706	0.004
	Transketolase inhibitor	0.706	0.005
	Formaldehyde transketolase inhibitor	0.709	0.010
	Aldehyde oxidase inhibitor	0.714	0.016
	Pseudolysin inhibitor	0.715	0.017
	Alcohol O-acetyltransferase inhibitor	0.703	0.005
	2.4-Dichlorophenol 6-monooxygenase inhibitor	0.701	0.003
	Glutathione thiolesterase inhibitor	0.713	0.016
	Amine dehydrogenase inhibitor	0.704	0.008
	Cytoprotectant	0.701	0.005
	Antineurotic	0.708	0.038
Limonene (GEO)	Carminative	0.961	0.001
	Retinol dehydrogenase inhibitor	0.934	0.000
	Antieczematic	0.896	0.005
	Alpha-pinene-oxide decyclase inhibitor	0.881	0.001
	Apoptosis agonist	0.816	0.007
	Antineoplastic	0.812	0.010
	CYP2C substrate	0.799	0.010
	Transcription factor NF kappa B stimulant	0.765	0.003
	Transcription factor stimulant	0.765	0.003
	UGT1A4 substrate	0.756	0.004
	Aspulvinone dimethylallyltransferase inhibitor	0.780	0.040
	Acetylcholine neuromuscular blocking agent	0.743	0.004
	Chemoprotective	0.740	0.003
	CYP2A6 inhibitor	0.721	0.003
	Alcohol dehydrogenase substrate	0.720	0.002
	Testosterone 17beta-dehydrogenase (NADP+) inhibitor	0.753	0.038
	CYP2J substrate	0.747	0.035
	Dermatologic	0.716	0.007
	CYP2C12 substrate	0.753	0.047
	Respiratory analeptic	0.716	0.014
	Immunosuppressant	0.714	0.015
	Ubiquinol-cytochrome-c reductase inhibitor	0.707	0.066

References

Abraham DJ. 2003. Burger's Medicinal Chemistry and Drug discovery. Chemotherapeutic Agents 5th edition.

Adefegha SA, Oboh G. 2012. *In vitro* inhibition activity of polyphenol-rich extracts from *Syzygium aromaticum* (L.) Merr. & Perry (Clove) buds against carbohydrate hydrolyzing enzymes linked to type 2 diabetes and Fe2+-induced lipid peroxidation in rat pancreas.Asian Pac. J. Trop. Biomed. 2(10): 774-781.

Adefegha SA, Oboh G, Omojokun OS, Jimoh TO, Oyeleye SI. 2016. *In vitro* antioxidant activities of African birch (*Anogeissus leiocarpus*) leaf and its effect on the α-amylase and α-glucosidase inhibitory properties of acarbose. J Taibah Univ Sci, 11: 236-242.

Agnish S, Sharma AD, Kaur I. 2022. Underutilized Plant *Cymbopogon pendulus* Derived Essential Oil Is Excellent Source of Bioactives with Diverse Biological Activities. Russ. Agricult. Sci. 48: 89-102.

Ahmed MU, Ibrahim, A, Dahiru NJ, Mohammed, S. 2020. Alpha Amylase Inhibitory Potential and Mode of Inhibition of Oils from *Allium sativum* (Garlic) and *Allium cepa* (Onion). Clin. Med. Insights Endocrinol. Diabetes, 13: 1179551420963106.

Ajiboye BO, Ojo OA, Fatoba B, Afolabi OB, Olayide I, Okesola MA, Oyinloye BE. 2019. *In vitro* antioxidant and enzyme inhibitory properties of the n-butanol fraction of *Senna podocarpa* (Guill. and Perr.) leaf. J Basic Clin Physiol Pharmacol, 31: 20190123.

Alema NM, Periasamy G, Sibhat GG, Tekulu GH, Hiben MG. 2020. Antidiabetic activity of extracts of *Terminalia brownii Fresen*. Stem bark in mice. J Exp Pharmacol, 12: 61-71.

Alraddadi BG, Shin HJ. 2022. Biochemical properties and cosmetic uses of Commiphora myrrha and Boswellia serrata. Cosmetics, 9(6): 119.

Amrita, Kaur, I, Sharma AD. 2023. Underutilized plant Cymbopogan martinii derived essential oil is excellent source of bioactives with diverse biological activities. Russ. Agric. Sci., 49(1): 100-117.

Anigboro AA, Avwioroko OJ, Ohwokevwo OA, Nzor JN. 2018. Phytochemical constituents, antidaibetic and ameliorative effects of *polyalthia longifola* leaf extracts in alloxan-induced diabetic rats. J. Appl. Sci. Environ. Manag. 22(6): 993.

Anigboro AA, Avwioroko OJ, Ohwokevwo OA, Pessu B, Tonukari NJ. 2021. Phytochemical profile, antioxidant, α-amylase inhibition, binding interaction and docking studies of *Justicia carnea* bioactive compounds with α-amylase. Biophysical chemistry, 269: 106529.

Apostolidis E, Kwon YI, Shetty K. 2007. Inhibitory potential of herb, fruit, and fungal-enriched cheese against key enzymes linked to type 2 diabetes and hypertensionInnov. Food Sci. Emerg. Technol., 8: 46-54.

Asmat U, Abad K, Ismail K. 2016. Diabetes mellitus and oxidative stress-A concise review. Saudi Pharm J., 24(5): 547-553.

Avwioroko OJ, Anigboro AA, Atanu FO, Otuechere CA, Alfred, MO, Abugo JN, Omorogie MO. 2020. Investigation of the binding interaction of α-amylase with *Chrysophyllum albidum* seed extract and its silver nanoparticles: a multi-spectroscopic approach. Chem. Data Collections, 100517.

Basak SS., Candan F. 2013. Effect of *Laurus nobilis* L. essential oil and its main components on α-glucosidase and reactive oxygen species scavenging activity. Iranian journal of pharmaceutical research: IJPR, 12(2): 367.

Bejarano E, Taylor A. 2019. Too sweet: problems of protein glycation in the eye. Experimental eye Res.. 178: 255-262

Bhaskarachary K, Joshi AK. 2018. Natural bioactive molecules with antidiabetic attributes: Insights into structure–activity relationships. Studies in Natural Products Chemistry 57: 353-388.

Bogavac MA, Perić TM, Mišković J, Karaman M. 2022. Antimicrobial and toxic effects of Boswellia Serrata Roxb. and Mentha piperita Linn. essential oils on vaginal inhabitants. Medicines, *9*(12): 62.

Ch'ng LZ, Barakatun-Nisak MY, Zukiman WZHW, Abas F, Wahab NA. 2019. Nutritional strategies in managing postmeal glucose for type 2 diabetes: A narrative review. *Diabetes & Metabolic Syndrome*, 13: 2339-2345.

Dalli M, Daoudi NE, Abrigach F, Azizi SE, Bnouham M, Kim B, Gseyra N. 2022. *In vitro* α-amylase and hemoglobin glycation inhibitory potential of *Nigella sativa* essential oil, and molecular docking studies of its principal components Front. Pharmacol. 13: 1036129.

de Macedo LM, Santos ÉMD, Militão L, Tundisi LL, Ataide JA, Souto EB, Mazzola PG. 2020. Rosemary (*Rosmarinus officinalis* L., syn *Salvia rosmarinus* Spenn.) and its topical applications: A review. *Plants*, *9*(5): 651.

Derosa G, Maffioli P. 2012. α-Glucosidase inhibitors and their use in clinical practice. Archives of Medical Science, 8: 899.

Derosa G, D'Angelo A, Maffioli P. 2020. Change of some oxidative stress parameters after supplementation with whey protein isolate in patients with type 2 diabetes. Nutr. 73: 110700.

El Moussaoui A, Mechchate H, Bourhia M, Es-safi I, Salamatullah AM, Alkaltham MS, Alyahya HK, Bousta D, Bari A. 2021. Glycemic control potential of chemically characterized extract from *Withania frutescens l.* Roots in severe diabetes-induced mice. Applied Sciences 11: 3998.

Elshama S, Abdalla ME, Mohamed AM. 2018. Role of Natural antioxidants in treatment of toxicity. *J Toxicol Anal*, *1*(1): 3.

Elwekeel A, El Amir D, Mohamed EI, Amin E, Hassan MH, Zaki MA. 2022. Characterization of Possible α-Glucosidase Inhibitors from *Trigonella stellata* Extract Using LC–MS and *In Silico* Molecular Docking. Plants, 11: 208.

Farombi EO, Awogbindin IO, Olorunkalu PD, Ogbuewu E, Oyetunde BF, Agedah AE, Adeniyi PA. 2020. Kolaviron protects against nigrostriatal degeneration and gut oxidative damage in a stereotaxic rotenone model of Parkinson's disease. Psychopharmacol., 1-12.

Goel RK, Singh D, Lagunin A, Poroikov V. 2011. PASS-assisted exploration of new therapeutic potential of natural products. Medi Chem Res. 20:, 1509–1514.

Hussain H, Al-Harrasi A, Al-Rawahi A, Hussain J. 2013. Chemistry and biology of essential oils of genus boswellia. *Evidence-based complementary and alternative medicine*, 140509.

Ismail SM, Hassan NA, Wahba TF, Shaker N. 2022. Chemical composition and bioactivities of Melaleuca alternufolia essential oil and its main constituents against *Spodoptera littoralis* (Boisaduval, 1833). *Bulletin of the National Research Centre*, *46*(1): 157.

Kazeem MI, Adamson JO, Ogunwande IA. 2013. Modes of inhibition of α-amylase and α-glucosidase by aqueous extract of *Morinda lucida* Benth leaf. BioMed research international, 2013: 527570.

Khan M, Liu H, Wang J, Sun B. 2020. Inhibitory effect of phenolic compounds and plant extracts on the formation of advance glycation end products: A comprehensive review. Food Res. Int. 130: 108933.

Khurana N, Ishar MPS, Gajbhiye A, Goel RK. 2011. PASS assisted prediction and pharmacological evaluation of novel nicotinic analogs for nootropic activity in mice. Eur. J. Pharmacol. 662: 22-30.

König J, Müller F, Fromm MF. 2013. Transporters and drug-drug interactions: important determinants of drug disposition and effects. Pharmacological Reviews, 65: 944-966.

Lolok N, Sumiwi SA, Muhtadi A, Susilawati Y, Hendriani R, Ramadhan DSF, Levita J, Sahidin I. 2022. Molecular docking and molecular dynamics studies of bioactive compounds contained in noni fruit (*Morinda citrifolia L.*) against human pancreatic α-amylase. Journal of Biomolecular Structure and Dynamics 40: 7091-7098.

McCoy RG, Lipska KJ, Van Houten HK, Shah ND. 2020. Association of cumulative multimorbidity, glycemic control, and medication use with hypoglycemia-related emergency department visits and hospitalizations among adults with diabetes. Journal of the American Medical Association Network Open 3: 1919099-1919099.

McCue P, Kwon YI, Shetty K. 2005. Antiαamylase, antiαglucosidase and antiangiotensin I converting enzyme potential of selected foods. Journal of Food Biochemistry, 29: 278-294.

Mir WR, Bhat BA, Rather MA, Muzamil S, Almilaibary A, Alkhanani M, Mir MA. 2022.Molecular docking analysis and evaluation of the antimicrobial properties of the constituents of *Geranium wallichianum D. Don* ex Sweet from Kashmir Himalaya. Scientific Reports, 12: 12547.

Nasab SB, Homaei A, Karami L. 2020. Kinetic of α-amylase inhibition by *Gracilaria corticata* and *Sargassumangustifolium* extracts and zinc oxide nanoparticles. Biocatalysis and Agricultural Biotechnology, 23: 101478.

Nieto G, Ros G, Castillo J. 2018. Antioxidant and antimicrobial properties of rosemary (*Rosmarinus officinalis*, L.): A review. *Medicines*, *5*(3): 98.

Nimse SB, Pal D. 2015. Free radicals, natural antioxidants, and their reaction mechanisms. *RSC advances*, *5*(35): 27986-28006.

Oboh G, Ademiluyi AO, Akinyemi AJ, Henle T, Saliu, JA, Schwarzenbolz U. 2012. Inhibitory effect of polyphenol-rich extracts of jute leaf (*Corchorus olitorius*) on key enzyme linked to type 2 diabetes (α-amylase and α-glucosidase) and hypertension (angiotensin I converting) *in vitro* . *Journal of functional foods*, *4*(2): 450-458.

Ogunyemi OM, Gyebi AG, Adebayo JO, Oguntola JA, Olaiya CO. 2020. Marsectohexol and other pregnane phytochemicals derived from *Gongronema latifolium* as α-amylase and α-glucosidase inhibitors: *in vitro* and molecular docking studies. SN Applied Sciences, 2: 1-11.

Otuechere CA, Adewuyi A, Oluwabayo T, Afolayan F, Avwioroko O, Abazuh U. 2020. Salubrious effects of a vermiculite–cellulose-based bionanocomposite on oxidative stress indices and histomorphology of male Wistar rats. Andrologia 52(1): 13426.

Rahmati-Joneidabad M, Alizadeh behbahani B. 2021. *Boswellia sacra* essential oil: Antioxidant activity and antifungal effect on some spoilage fungi causing strawberry rot. FSCT, 18(114): 25-34.

Reza AA, Haque MA, Sarker J, Nasrin MS, Rahman MM, Tareq AM, Khan Z, Rashid M, Sadik MG, Tsukahara T, Alam AK. 2021. Antiproliferative and antioxidant potentials of bioactive edible

vegetable fraction of Achyranthes ferruginea Roxb. in cancer cell line. *Food Science & Nutrition*, *9*(7): 3777-3805.

Sharma AD, Inderjeet K,,Ravneet K, Amrita C. 2023a. Essential oil from *Melaleuca alternifolia*: Aromatic profiling, phytochemical analysis and assessment of diverse biological activities. Russ. Agricult. Sci. 49: 558–574.

Sharma AD,· Inderjeet K, Amrita,Ranjna D. 2023b. Phytochemical profile using GC-FID and diverse in vitro biological activities of essential oil extracted from *Boswellia serrata*. Arabian Journal of Medicinal and Aromatic Plants, 9: 1-37.

Sharma AD, Ravindresh C, Puneet J, Inderjeet K, Amrita C,,Retika R.· 2023c. Preparation, characterization and in vitro bioassays of nanoemulsions prepared from essential oil extracted from *Rosmarinus officinalis* L. Bionanoscience. BioNanoScience 13(4): 1-21.

Siddique S, Parveen Z, Butt A, Chaudhary MN, Akram M. 2017. The essential oil of *Melaleuca armillaris* (Sol. ex Gaertn.) Sm. leaves from Pakistan: A potential source of eugenol methyl ether. *Inds. Crops Prod.*, *109:* 912–917.

Smita K, Manjunath K, Sitikantha S. 2018. Evaluation of α-glucosidase inhibitory potential of methanolic leaf extract of *Ocimum canum*. International Journal of Pharmacy and Pharmaceutical Sciences, 10: 126-131.

Srimai V, Ramesh M, Satya Parameshwar K, Parthasarathy T. 2013. Computer-aided design of selective Cytochrome P450 inhibitors and docking studies of alkyl resorcinol derivatives. Medicinal Chemistry Research, 22: 5314-5323.

Unuofin JO, Lebelo S.L. 2020. Antioxidant effects and mechanisms of medicinal plants and their bioactive compounds for the prevention and treatment of type 2 diabetes: an updated review. Oxid Med Cell Longev., 2020: 1356893.

Veber DF, Johnson SR, Cheng HY, Smith BR, Ward KW, Kopple KD. 2002. Molecular properties that influence the oral bioavailability of drug candidates. Journal of Medicinal Chemistry, 45: 2615-2623.

Viuda-Martos M, Ruiz Navajas Y, Sánchez Zapata E, Fernández-López J, Pérez-Álvarez JA. 2010. Antioxidant activity of essential oils of five spice plants widely used in a Mediterranean diet. *Flavour Frag J.*, 25: 13-19.

Wang BL, Pan DQ, Kou SB, Lin ZY, Shi JH. 2020. Exploring the binding interactionbetween bovine serum albumin and perindopril as well as influence of metal ions usingmulti-spectroscopic, molecular docking and DFT calculation. Chem. Phys., 110641.

Wu C, Liu Y, Yang Y, Zhang P, Zhong W, Wang Y, Wang Q, Xu Y, Li M, Li X, Zheng M. 2020. Analysis of therapeutic targets for SARS-CoV-2 and discovery of potential drugs by computational methods. Acta Pharmaceutica Sinica B, 10: 766-788.

Zheng Y, Yang W, Sun W, Chen S, Liu D, Kong X, Tian J, Ye X. 2020. Inhibition of porcine pancreatic α-amylase activity by chlorogenic acid. J. Func. Foods, 103587.